J. ISSS Vol. **2** No. 2, pp. 18-26, Sept 2012.
REGULAR PAPER

A Comparison of Burst Strength and Linearity of Pressure Sensors having Thin Diaphragms of Different Shapes

Vidhya Balaji and K.N. Bhat
Centre for Nano Science and Engineering,
Indian Institute of Science, Bangalore-560012
Corresponding author email:vidbalaji2000@yahoo.com

Keywords:

Burst strength, Linearity,
Pressure sensor,
Stress Distribution,
Diaphragm

Abstract

The shapes of diaphragms most commonly used for Micro Electro Mechanical Systems (MEMS) applications are square, circular and rectangular. The aim of this analysis is to highlight the distinctions among these three shapes with respect to burst strength and linearity and to identify the shape with the best characteristics for a given diaphragm thickness and width. A Finite Element (FE) Analysis carried out with Coventorware software is used to simulate the stress distribution for a range of applied pressure on the diaphragm. We consider single-crystal silicon <100> as the diaphragm material. Anisotropic wet etch is the means of fabrication for the rectangular and square diaphragms and for the circular diaphragm it is dry etching. We show that the circular diaphragm gives us both good linearity characteristics and the highest burst stress tolerance characteristics.

1. Introduction

MEMS devices are widely used in the area of sensors, for eg., pressure sensors, optical sensors, microphones, actuators, etc.. Diaphragms, being the primary mechanical components of these devices, are fabricated by bulk or surface micromachining silicon, which is the most popular material for micromachined sensors. Three diaphragm shapes, circular, square and rectangular are used depending on the application. The choice of diaphragm shape is based mainly on the fabrication process used for realizing it. In addition, it depends upon several other factors such as the applications and distribution of the required stress field. In most cases, square and rectangular shapes are preferred because of the ease of fabrication by the anisotropic wet chemical etching of silicon. On the other hand, the fabrication of circular diaphragms in silicon is possible by Deep Reactive Ion Etching (DRIE). Some of the comparison studies reported in the literature [Khakpour *et al.,* 2010, Lee *et al.*, 2008] on the effect of the three diaphragm shapes with respect to deflection, stress and vibration frequency suggest that square diaphragms are useful for tactile sensors whereas rectangular diaphragms are suitable where packaging constraints limit the width vis-à-vis the length. It has also been reported that the circular diaphragm is optimal [Lee *et al.*, 2008] in the case of structures like microphones because of the largest center deflection for a given area. Also, the circular diaphragm has the lowest stress on its edges in comparison to the other shapes for the same applied pressure. The design criteria for surface micromachined pressure sensors with square and circular diaphragms have been reported in the literature [Lin and Yun,1998], [Lin *et al.,*1999]. However, the focus in those papers has been on the location of piezoresistors to achieve the best sensitivity and linearity. The combined effects of the area and the geometry of the diaphragm on linearity and reliability criteria based

Available online at www.isssonline.in/journal/02paper08pdf Paper presented at the Fifth ISSS National Conferece on MEMS, Smart Materials, Structures and Systems, September 21-22, 2013 (ISSS NC 5), Karpagam University, Coimbatore, India.

on the burst pressure have not been reported in the literature.

In this paper, we present the results of a detailed Finite Element (FE) analysis of the three diaphragm types having rectangular, square, and circular shapes, and compare the stress distribution across these three types of diaphragms and arrive at their relative merits in terms of the maximum operation pressure governed by the burst pressure and linearity considerations. Using the Coventorware FE analysis tool, we demonstrate quantitatively the importance of choosing the appropriate shape and area of the diaphragm to optimize the burst pressure and the linearity of the pressure sensor output.

2. Theory

2.1 Burst pressure

As the applied pressure on the diaphragm increases, the stress on the diaphragm increases correspondingly. As a result, when the maximum stress on any portion of the diaphragm exceeds the yield strength of the diaphragm material, the diaphragm will burst. While this burst pressure governs the maximum operating pressure of a pressure sensor, the linearity of operation determines the maximum pressure up to which the sensor can be used within the limits of the specified accuracy. The burst pressure is decided by a number of factors including diaphragm shape, thickness, lateral dimensions, rupture stress of the material and diaphragm surface roughness [Henning *et al.*, 2004]. Although theoretically, the yield strength is 7 GPa for silicon, due to the influence of the aforementioned factors, the rupture stress has been found to be considerably lower. In fact, with anisotropically etched diaphragms, burst stresses of the order of even 300 MPa have been observed [http:// design.caltech.edu /Research/MEMS/ siliconprop.html]. By making minor modifications to the shape of the diaphragm through fabrication steps, we can increase its yield strength, thereby enhancing its robustness. For example, rounding of the corners of square and rectangular diaphragms through DRIE is one such technique that has been used to achieve this objective [Ngo *et al.*, 2008]. Studies have shown that burst pressure increases by over 50% in devices with lateral radii of curvature of 0.2 compared to those with no measurable curvature [Pourahmadi *et al.*, 1991]. Other than experimental tests to determine the burst pressure, FEM sub-modeling is a technique that has been used to find the burst strength of conventional diaphragms [Pourahmadi *et al.*, 1990]. The maximum stress being concentrated at a very small region close to the diaphragm edge, it has been demonstrated that sub-modeling for region refinement gives a good estimate of the value. FEM data fitting has also provided an approximate expression for burst pressure, $P_{b,}$ for a square diaphragm [Bistue *et al.*, 1997]:

$$P_b = \frac{3.4\sigma_{max} h^2}{(1-\upsilon^2)A} \qquad (1)$$

where σ_{max} is the maximum stress, 'h' is the diaphragm thickness, υ is Poisson's ratio and A is the diaphragm area. One of the design criteria for the diaphragm based pressure sensor is that the burst pressure should be about five times the maximum operating pressure [Bhat, 2007].

ó$_{max}$ for the circular and square diaphragms are given by equations 2 and 3 respectively. They show that compared to a circular diaphragm with the same characteristic length ('d' diameter vs. 'a' edge length), the square diaphragm will have a larger maximum stress for the same applied pressure. Hence, the square diaphragm is more sensitive, but will have a lower threshold before bursting [Plotkowski *et al.*, 2012].

$$\sigma_{max} = \frac{3\,p\,d^2}{4t^2} \qquad (2)$$

$$\sigma_{max} = \frac{0.308\,p\,a^2}{t^2} \qquad (3)$$

2.2 Linearity of pressure sensor output

The second criterion for the maximum operating pressure of a piezoresistive pressure sensor is decided by the extent of linearity of the sensor output. This in turn depends upon the diaphragm deflection compared to its thickness. External factors like temperature also affect linearity although it is more of a consideration in highly sensitive applications. Linearity error expresses the amount of deviation of the output from the linear

curve(straight line) as a percentage of full-scale output and is an important specification of diaphragm deflection.

The relationship between applied pressure and linearity of diaphragm deflection is represented by the load-deflection equation for thin diaphragms. The expression contains both linear and non-linear terms.

For a flat, square diaphragm the relation is given by [Wang *et al.*, 2004]

$$\frac{P a^4}{E h^4} = \frac{4.2}{(1-\upsilon^2)}\left(\frac{d}{h}\right) + \frac{1.58}{1-\upsilon}\left(\frac{d}{h}\right)^3 \qquad (4)$$

where

P - the applied pressure in Pascals,

d - the deflection at the center of the diaphragm,

a - the half side length,

E - Young's modulus,

h - the diaphragm thickness,

υ - Poisson's ratio of the diaphragm material

When the deflection 'd' is less than 25% of the diaphragm thickness 'h', the nonlinear second term in equation (4) is negligible and hence the deflection varies as a linear function of 'd' as described by the first linear term. As a general rule, the deflection 'd' of the diaphragm at the center must be no greater than the diaphragm thickness; and for linearity in the order of 0.3%, should be limited to one quarter the diaphragm thickness.

In the case of a flat, circular diaphragm with clamped edges, the pressure-deflection relation assumes the following form [van Mullem *et al.*, 1991]:

$$\frac{P a^4}{E h^4} = \frac{16}{3(1-\upsilon^2)}\left(\frac{d}{h}\right) + \frac{7-\upsilon}{3(1-\upsilon)}\left(\frac{d}{h}\right)^3 \qquad (5)$$

Here, all the terms are the same as defined in equation (4) except the term, 'a', which is the radius of the diaphragm in this case. As in the square diaphragm case, the first term refers to the small deflection or linear region and the second term refers to the large deflection or non-linear region.

Similarly for the case of a flat, rectangular diaphragm with sides 2a and 2b ($a \leq b$) [Tabata *et al.*, 1989]:

$$P = \frac{C_1 h \sigma d}{a^2} + \frac{C_2 h E d^3}{a^4} \qquad (6)$$

Here, all the terms are the same as defined in equation (4) and 'σ' is the residual stress. C_1 and C_2 are the constant values determined by the aspect ratio and Poisson's ratio. C_1 and C_2 are 3.04 and 1.83 respectively for the length 'b' to width 'a' aspect ratio b/a= 1, i.e., square diaphragm. As b/a increases, C_1 decreases to approach the constant value of 1.52.

The transition between the linear and non-linear regions depends on the deflection and a variation can be observed between the three shapes for a given diaphragm dimension.

3. FE Analysis of the three Dia-Phragm Shapes

We have carried out an FE analysis of the three diaphragm shapes using Coventorware to determine the stress linearity pattern on the diaphragm and its burst pressure characteristics in relation to applied pressure. As was mentioned before, the actual yield strength for the silicon diaphragm deviates significantly from the theoretical 7 GPa and the FE modeling is used to determine the realistic values. Our approach is to apply a range of pressures between low and high (of the order of maximum non-destructive applied pressure) and analyze the stress distribution in the three shapes, namely, circular, square and rectangular represented in Fig. 1.

Wet etching of the backside is used for the fabrication of square and rectangular diaphragms. For the circular diaphragms, DRIE is the etching method considered, and the diaphragm dimensions are chosen as follows:

Square : 400 μm x 400 μm;

Rectangular : 400 μm x 314 μm;

Circular : 400 μm diameter;

In all cases, the diaphragm thickness is h = 10 μm.

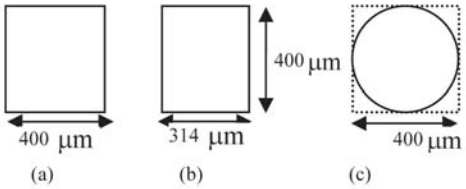

Figure 1. Dimensions of the diaphragms having, (a) Square (b) Rectangular and (c) Circular shapes

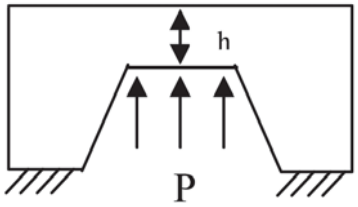

Figure 2. Cross section of the diaphragm

For the purpose of comparing the stress distribution on the diaphragm, the side length, 400 µm, of the square diaphragm is chosen to be the same as the diameter (400 µm) of the circular diaphragm. The dimensions of the rectangular diaphragm are chosen to be 400 µm x 314 µm so that its area is equal to that of the circular one. At the same time, one side length of the rectangular diaphragm is maintained at 400µm so that it is equal to that of the square. In our simulation study, pressure, P, ranging from 0.6 MPa to 25 MPa is applied from the rear of each diaphragm as in Fig.2 for all the three cases shown in Fig.1, and the stress distribution across the width as well as at the corners of the diaphragm are studied.

4. Modelling in Conventorware

The mesh model in the simulation has hexahedral-shaped constituent elements (mapped bricks for square and circular diaphragms and Manhattan bricks for the rectangular diaphragm). These elements gave us the most optimal analyzer outputs for the respective diaphragm shapes. Varying the 3D element size between 50 microns and 10 microns, we were able to observe the convergence of stress and displacement.

For determining the stress at corners, we specified smaller element sizes at the boundaries between the diaphragm and the substrate. A tetrahedral element shape was used in this case. The accuracy of the values can be increased through this approach.

5. Results of FE Analysis

5.1 Stress distribution across diaphragm width

The top-surface stress profile across the width along a line through the center of the diaphragm is shown in figures 3-5 for the circular, square, and rectangular diaphragms, respectively, for a pressure range between 0.6 MPa to 25 MPa applied on the rear of the diaphragm of thickness h=10 µm. Directional stress along the axis parallel to the width is considered here. The positive and negative values indicate tensile and compressive stress, respectively.

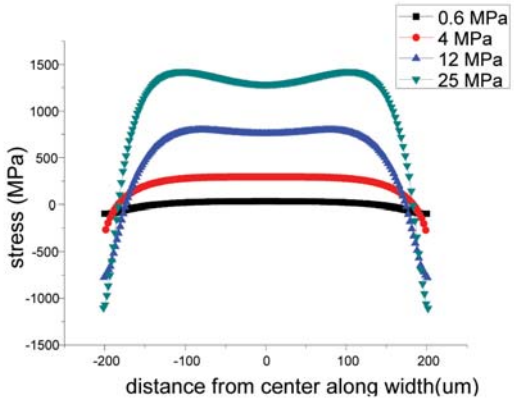

Figure 3. Stress distribution on the top surface along the diameter of circular diaphragm

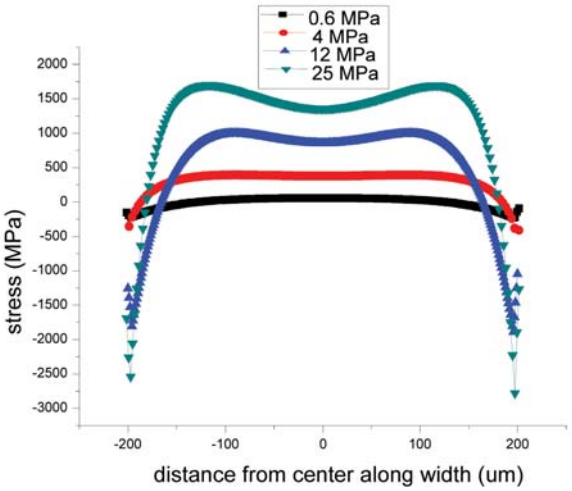

Figure 4. Stress distribution across the width along the line passing through the center of square diaphragm

Referring to Figures 3 and 4, it may be noted that the resultant stress at the center of the diaphragm for the square and circular diaphragms displays a similar pattern, and the stress peak at

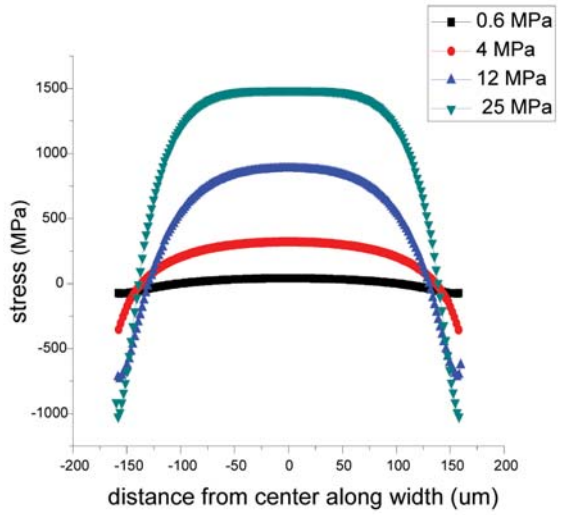

Figure 5. Stress distribution across the width (314 microns) along the line passing through the center of rectangular diaphragm

the center begins to dip at higher applied pressure, giving rise to an apparent "two-peak" effect with the maximum values shifted to either side of the center, indicating that nonlinearity sets in the diaphragm behavior at higher pressures. However, in the rectangular case, the stress becomes increasingly uniform across the width displaying greater stress tolerance for applied pressure. Further, it can be seen that the compressive stress is highest near the edge of the square diaphragm (Fig. 4) compared to the circular (Fig. 3) and rectangular diaphragms (Fig. 5), indicating that the circular and rectangular diaphragms will have a higher burst tolerance when compared to the square.

Next, we compare the magnitude of the stress at the center of the diaphragm with that at the edge for the entire range of pressure to obtain an insight into the linearity aspects and identify conditions that indicate burst pressures for each of the three shapes.

5.2 Linearity behavior

The maximum deflection, d, of the diaphragm estimated from the simulation results shown in Fig. 6 illustrates that a linear relationship exists up to pressure, P=1MPa. Consequently, the stress response at the middle of the diaphragm edge as well as at the diaphragm center are also linear in the pressure range 0.1 MPa to 1MPa as shown in Fig.7(a) and Fig.7(b) for all the three cases.

By analyzing the linearity error over a full-scale output corresponding to a pressure of 2 MPa, we can find out the relative linearity of the three diaphragms. We have used the displacement values for calculating the error in place of the output voltage normally used. This is justified, as the output voltage is proportional to the displacement. We estimate the nonlinearity using the formula:

$$NL_i = \frac{d(p_i) - \frac{d(p_m)}{p_m} \times p_i}{d(p_m)} \times 100\ \%$$

where $d(p_i)$ is the displacement when the applied pressure is p_i

p_m is the maximum pressure in the range

The linearity error thus estimated for the three diaphragm shapes are given below:

Square : 4.3%
Rectangular : 3.5%
Circular : 4%

The rectangular and square diaphragms respectively show the minimum and maximum linearity errors.

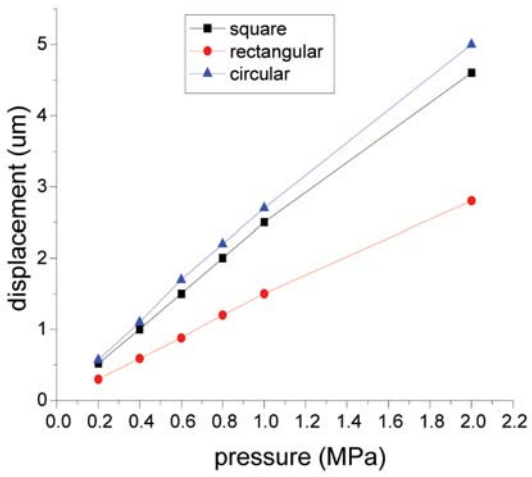

Figure 6. Displacement at center of diaphragm (<= 2 MPa)

A further analysis of these figures brings out several interesting features. (i) Referring to Fig.6, the center-deflection in the rectangular diaphragm is lower compared to the circular and square diaphragms. This is attributed to its narrower width

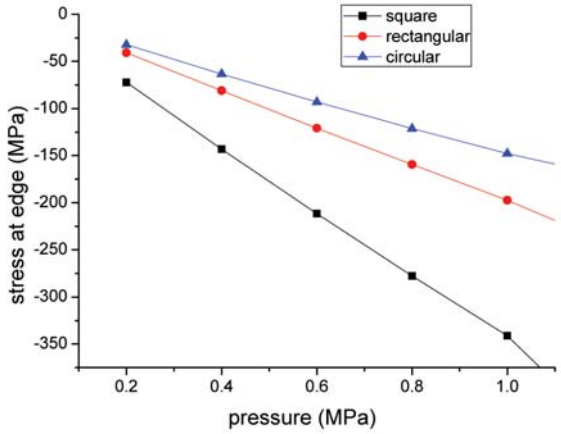

Figure 7(a). Stress magnitude at the edge of diaphragm for pressure <1 MPa

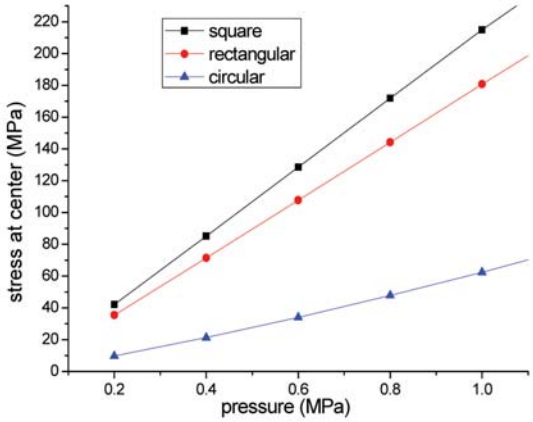

Figure 7(b). Stress magnitude at center of the diaphragm for pressure <1 MPa

of 314 microns as compared to the 400-micron width in the square and circular diaphragms. (ii) From the figures 7(a) and 7(b), it can be seen that the magnitudes of stress at the center as well as at the edge are lowest in the circular diaphragm case, indicating that the circular diaphragm can be used over a wider range of pressures and can withstand higher pressures. (iii) It can be further seen from Fig. 7(a) that the stress at the edge of the diaphragms, where we place the resistors, is comparable in the circular and rectangular diaphragms whose areas are the same, whereas the square diaphragm whose area is larger shows higher values of stress even though the width is the same as that of the circular diaphragm.

The diaphragm displacement corresponding to various pressure values can also be used to demonstrate the reliability of the FE analysis. From equations 4, 5 and 6, we calculate the displacement at pressures P=0.6 MPa, P=4 MPa and compare it with the values obtained through FEA. A relatively higher deviation between the values calculated from the equation and the FEA results can be observed for the P= 4MPa case, which can be explained by the higher non-linearity as the pressure is increased.

Table 1. Maximum central displacement of the square, rectangular and circular diaphragms for P=0.6MPa

Square		Rectangular		Circular	
Eqn.	FEA	Eqn.	FEA	Eqn.	FEA
1.49 μm	1.5 μm	0.8 μm	0.88 μm	1.2 μm	1.7 μm

Table 2. Maximum central displacement of the square, rectangular and circular diaphragms for P=4MPa

Square		Rectangular		Circular	
Eqn.	FEA	Eqn.	FEA	Eqn.	FEA
8.2 μm	9.34 μm	5.4 μm	5.32 μm	7.6 μm	8.2 μm

5.3 Comparison of stress at center and edge of diaphragm

In order to ascertain the nature of stress variation over a wide range of pressures, we determine the stress response at the center of the diaphragm and at the edge of the diaphragm over the entire pressure range of 1 MPa to 25 MPa. The results are presented in figures 8(a) and 8(b). As a whole, we can see that in both the locations of the diaphragm, the circular diaphragm displays the lowest stress throughout the pressure range

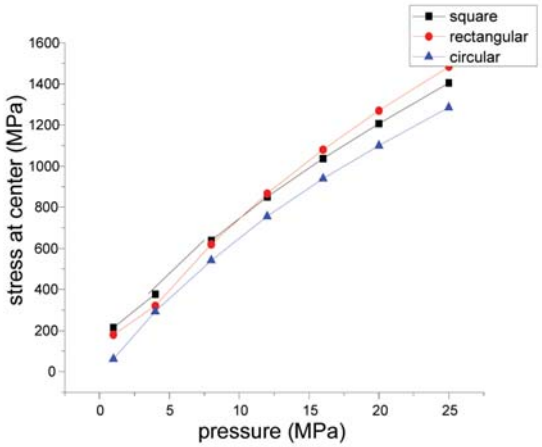

Figure 8(a). Stress magnitude at center of diaphragm, over a wide range of pressures.

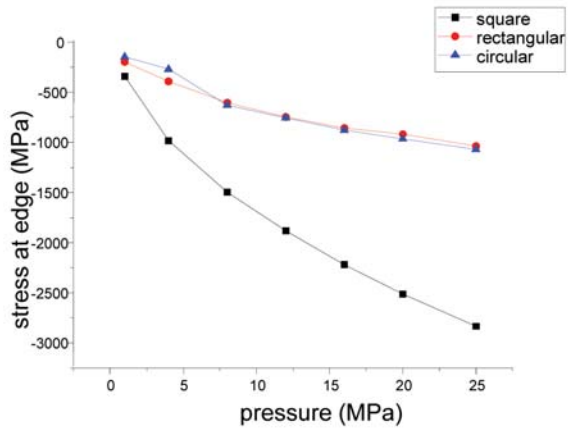

Figure 8(b). Stress magnitude at edge of the diaphragm over a wide range of pressures.

compared to the square and rectangular cases. Comparing the results in Fig. 8(a) and Fig. 8(b), it can be seen that as the applied pressure increases, the magnitude of stress at the center becomes greater than that at the edges for the rectangular and circular cases, indicating that the burst pressure may be governed by the stress at the center of the diaphragm. The highest pressure tolerance is exhibited by the circular diaphragm with a pressure of nearly 19 MPa required to develop a stress level of 1 GPa at the center of the diaphragm.

Next, we compare the stress at the corners of the diaphragms with respect to that observed at the edges and estimate the burst pressures.

5.4 Comparison of burst pressures

For the square and rectangular diaphragms, the stress magnitudes at their four corners are analyzed to determine the burst pressure. Since the circular diaphragm mesh model is actually a square area that circumscribes the circle, we measure the stress at those points on the circumference of the circle coinciding with the edges of the square. (Since Coventorware does not provide for using circular planes for partitioning the mesh model, a square plane was used to select the diaphragm surface.) The stresses at the accessible points were used to determine the bursting threshold. When the stress magnitude is of the order of GPa and the stress magnitude at the center of the diaphragm is greater than that at the edges, we can assume that burst conditions have been reached.

The resultant stress along the diagonal direction was estimated for the square and rectangular diaphragms at the four corners using the X and Y stress components. For the circular diaphragm, the stress along the radial line at a point on the circumference was considered, as indicated in Fig.9. Fig.10 shows the comparison of corner stresses for the three types of diaphragms. Considering a theoretical maximum rupture stress to be approximately 1 GPa as shown by the horizontal dotted line, it can be seen from Fig.10 that the burst pressure of the square diaphragm is around 6 MPa and that of the rectangular diagram is close to 16 MPa, while the burst pressure of the circular diaphragm is 23 MPa. At this stage, it is interesting to note that if the analytical equation (1) is used to estimate the burst pressures, assuming σ_{max} = 1GPa, the burst pressure values for the rectangular and circular diaphragm turn out to be equal to each other, whereas the simulation results show that they are considerably different from each other. This effect may have occurred because the aspect ratio of the rectangular diaphragm has not been considered in the burst pressure equation (1).

From the simulation results, comparing the square and rectangular diaphragms, we get a better burst pressure performance for the latter as the area is smaller. When comparing the rectangular and circular diaphragms having the same areas, the circular has a higher burst threshold. Consequently, the circular diaphragm has the highest-pressure tolerance, as expected.

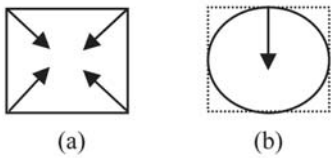

Figure 9. Stress component locations considered for burst pressure estimation for (a) square and rectangular and (b) circular diaphragm

6. Conclusions

We have considered three common diaphragm shapes and analyzed their linearity and burst pressure characteristics with FE analysis. Keeping the same diaphragm width in the case of square vs. circular and equal area in the case of rectangular vs. circular, we have shown that although the rectangular diaphragm has the most uniform

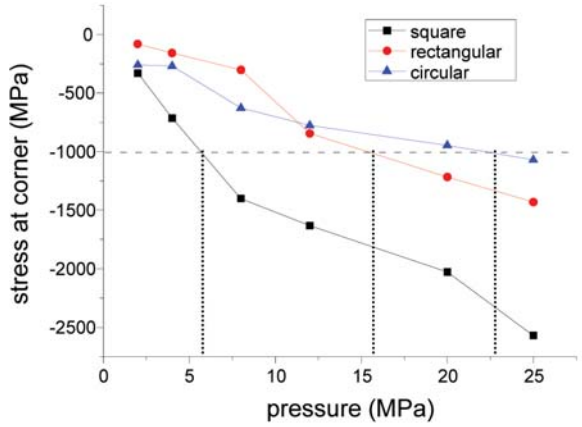

Figure 10. Stress magnitude at corner of diaphragm: The dotted horizontal line shows the critical maximum stress of 1000MPa. The dotted vertical lines show the corresponding burst pressures for the three cases.

linearity characteristics over a wide range of applied pressures, the circular diaphragm gives us both good linearity characteristics and the highest burst stress tolerance characteristics. The circular shape would be the most useful at higher applied pressures where high stress is an important limitation.

Acknowledgments

The authors wish to thank the Centre for Nano Science and Engineering at the Indian Institute of Science for providing the necessary tools for carrying out the study.

References

Bhat K.N., 2007, "Silicon Micromachined Pressure Sensors", Journal of Indian Institute of Science,Vol.87,125

Bistue G., Elizalde J.G. *et al*., 1997, "A Design Tool for pressure microsensors based on FEM simulations", Sensors and Actuators, A 62, 591-594.

Henning A.K., Patel S., Selser M., Cozad B.A., 2004, "Factors Affecting Silicon Membrane Burst Strength", Proc. of SPIE, Vol. 5343, 145-153.

Khakpour R., Mansouri R.M.S., Bahadorimehr A.R., 2010, "Analytical Comparison for Square, Rectangular and Circular Diaphragms in MEMS Applications", International Conference on Electronic Devices, Systems and Applications(ICEDSA2010), 297-299.

Lee W.S., Lee S.S., 2008, "Piezoelectric Microphone built on Circular Diaphragm", Sensors and Actuators, A 144, 367-373.

Lin L. *et al*.,1998,"Design,Optimization & Fabrication of Surface Micromachined Pressure Sensors," Journal of Mechatronics, Vol.8, 505- 519.

Lin L. et al,1999, "A Simulation Program for the Sensitivity and Linearity of Piezoresistive Pressure Sensors," I IEEE /ASME Journal of EEE/ASME Journal Of MEMS, Vol. 8, 514-522.

Mullem C.J. van, Gabriel K.J., Fujita H., 1991, "Large Deflection Performance of Surface Micromachined Corrugated Diaphragms", IEEE International Conference on Solid-State Sensors and Actuators, 1014-1017.

Ngo H.-D., Tham A.–T., Simon M., Obermeier E., 2008,"Corner Rounding to strengthen silicon pressure sensors using DRIE", IEEE Sensors Conference, 1576-1579.

Plotkowski A., Dr. Jiao L., Dr. Barakat N., 2012, "Design and Computational Analysis of Diaphragm-based Piezoresistive Pressure Sensors For Integration into Undergraduate Curriculum", American Society for Engineering Education

Pourahmadi F., Barth P., Petersen K., 1990, "Modeling of thermal and mechanical stresses in Si microstructures", Sensors and Actuators, A21-A23, 850-855.

Pourahmadi,F., Gee D., Petersen K., 1991, "The effect of Corner Radius of Curvature on the mechanical strength of micromachined single-crystal silicon structures," Solid-State Sensors and Actuators, Digest of Technical Papers, TRANSDUCERS '91, 197-200

Tabata O. *et al*., 1989,"Mechanical Property Measurements of Thin Films using load-deflection of composite rectangular diaphragms", Sensors and Actuators, Vol. 20, 135-141.

Wang X., Li B., Lee S., Sun Y., Roman H.T., Chin K., Farmer K.R.," 2004, A New Method to Design Pressure Sensor Diaphragm", NSTI-Nanotech, Vol. 1, 324-327.

http://design.caltech.edu/Research/MEMS/siliconprop.html

Vidhya Balaji received a Bachelor of Engineering degree in Electronics and Communications Engineering from the Regional Engineering College, Tiruchirapalli, India, in 2000 and a Masters in Technology majoring in VLSI Systems from the National Institute of Technology, Tiruchirapalli, India, in 2004. She has 8 years of work experience in domains such as DSL technology, satellite sub-systems design, encoder design and system verification. Her research interests include MEMS/NEMS design and fabrication, VLSI systems and nanotechnology.

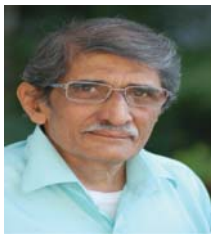

Prof K. N. Bhat is an alumnus of IISc, Bangalore, IIT Madras, and RPI, Troy, NY. His teaching and research interests include micro and nano electron devices, silicon and GaAs VLSI, MEMS technology, solar cells and power devices. He has served as faculty member of the EE Department at IIT Madras at Chennai, India and at the University of Washington Seattle (USA) and taught several courses both at the UG and PG levels. He has guided and mentored several Ph.D and MS research scholars and published extensively in International Journals and Conference Proceedings. His lecture series on high speed devices is now available in the YOUTUBE. He has carried out pioneering work in the MEMS area in India. He is a co-author of the books: "Micro and Smart Systems–Technology and Modelling" (2012) John Wiley and Sons (USA)., "Fundamentals of Semiconductor Devices" (2007) Tata McGraw-Hill. After superannuation and retirement from IIT Madras in the year 2006, he has been a Visiting Professor at the Centre for Nano Science and Engineering, Indian Institute of Science, Bangalore, where he has been teaching courses on nanoelectronics and MEMS technology, and mentoring research scholars, and coordinating major projects on MEMS-based pressure sensors for industrial, aerospace, and biomedical applications. Prof K.N. Bhat is a Fellow of the INAE.